

Tissue-specific expression atlas of murine mitochondrial tRNAs

Received for publication, February 5, 2021, and in revised form, July 4, 2021. Published, Papers in Press, July 13, 2021.
<https://doi.org/10.1016/j.jbc.2021.100960>

Qiufen He^{1,2}, Xiao He^{1,2}, Yun Xiao², Qiong Zhao², Zhenzhen Ye², Limei Cui², Ye Chen^{1,2,3,*}, and Min-Xin Guan^{1,2,3,4,5,*} 

From the ¹Division of Medical Genetics and Genomics, The Children's Hospital, Zhejiang University School of Medicine and National Clinical Research Center for Child Health, Hangzhou, Zhejiang, China; ²Institute of Genetics, Zhejiang University School of Medicine, Hangzhou, Zhejiang, China; ³Zhejiang Provincial Key Lab of Genetic and Developmental Disorders, Zhejiang University, Hangzhou, Zhejiang, China; ⁴Key Lab of Reproductive Genetics, Center for Mitochondrial Genetics, Ministry of Education of PRC, Zhejiang University, Hangzhou, Zhejiang, China; ⁵Division of Mitochondrial Biomedicine, Zhejiang University-University of Toronto Joint Institute of Genetics and Genome Medicine, Hangzhou, Zhejiang, China

Edited by Karin Musier-Forsyth

Mammalian mitochondrial tRNA (mt-tRNA) plays a central role in the synthesis of the 13 subunits of the oxidative phosphorylation complex system (OXPHOS). However, many aspects of the context-dependent expression of mt-tRNAs in mammals remain unknown. To investigate the tissue-specific effects of mt-tRNAs, we performed a comprehensive analysis of mitochondrial tRNA expression across five mice tissues (brain, heart, liver, skeletal muscle, and kidney) using Northern blot analysis. Striking differences in the tissue-specific expression of 22 mt-tRNAs were observed, in some cases differing by as much as tenfold from lowest to highest expression levels among these five tissues. Overall, the heart exhibited the highest levels of mt-tRNAs, while the liver displayed markedly lower levels. Variations in the levels of mt-tRNAs showed significant correlations with total mitochondrial DNA (mtDNA) contents in these tissues. However, there were no significant differences observed in the 2-thiouridylation levels of tRNA^{Lys}, tRNA^{Glu}, and tRNA^{Gln} among these tissues. A wide range of aminoacylation levels for 15 mt-tRNAs occurred among these five tissues, with skeletal muscle and kidneys most notably displaying the highest and lowest tRNA aminoacylation levels, respectively. Among these tissues, there was a negative correlation between variations in mt-tRNA aminoacylation levels and corresponding variations in mitochondrial tRNA synthetases (mt-aaRS) expression levels. Furthermore, the variable levels of OXPHOS subunits, as encoded by mtDNA or nuclear genes, may reflect differences in relative functional emphasis for mitochondria in each tissue. Our findings provide new insight into the mechanism of mt-tRNA tissue-specific effects on oxidative phosphorylation.

Transfer RNAs (tRNA) function as adapter molecules that decode messenger RNAs (mRNAs) during protein translation by delivering amino acids to the ribosome. In mammal mitochondria, 22 tRNAs (mt-tRNA), together with two rRNAs and

13 mRNA coding 13 structural components of oxidative phosphorylation system (OXPHOS), are encoded by own mitochondrial genome (mtDNA) (1–4). The mtDNA produces the polycistronic heavy (H)- and light (L)-strand transcripts that are catalyzed by mitochondrial transcription machinery (5–8). The H-strand transcripts contain 12S rRNA, 16S rRNA, 12 mRNAs, and 14 tRNAs including tRNA^{His}, tRNA^{Lys}, and tRNA^{Leu(UUR)}, while L-strand transcripts harbor ND6 mRNA and eight tRNAs including tRNA^{Gln} and tRNA^{Ser(UCN)} (5–10). These polycistronic transcripts are then processed resulting in the release of 13 mRNAs, 2 rRNAs, and 22 tRNAs, which are catalyzed by RNase P and RNase Z, respectively (11–13). The formation of functional mt-tRNAs for the synthesis of 13 mtDNA encoding polypeptides requires extensive base modifications, CCA addition, and aminoacylation (14–18). Transcription control of mt-tRNA genes in the mammalian tissues plays an important role in specific oxidative phosphorylation capacities required to satisfy their metabolic and energetic demands (19–22). However, little is known about the variations in the expression levels or physiological conditions of mt-tRNAs in differing types of both human and mouse tissues.

The abundance, nucleotide modification, and aminoacylation of tRNAs may reflect the tissue-specific differences in mitochondrial number, morphology, activity, and biogenesis (23, 24). In the present investigation, we performed systematic analysis of mt-tRNA expressions from mouse-derived brain, heart, liver, skeletal muscle, and kidney. The steady-state levels of 22 mt-tRNAs among these five tissue types were examined using tRNA Northern blot analysis (25, 26). The nucleotide modifications of tRNAs were assessed for the levels of 2-thiouridine modification at position U34 in tRNA^{Lys}, tRNA^{Glu}, and tRNA^{Gln} by isolating total mitochondrial RNAs from these tissues and then qualifying 2-thiouridine modifications by retardation of electrophoresis mobility in polyacrylamide gels containing *N*-acryloylamino phenyl mercuric chloride (27–29). Furthermore, we examined the aminoacylation levels of tRNAs using electrophoresis in an acidic urea polyacrylamide system to separate uncharged tRNA species from

* For correspondence: Min-Xin Guan, gminxin88@zju.edu.cn; Ye Chen, yechency@zju.edu.cn.

Tissue-specific expression of murine mitochondrial tRNA

the correspondingly charged tRNAs among these tissues (18, 30). Moreover, we investigated the tissue-specific expression of 14 mitochondrial tRNA synthetases (mt-aaRS) and OXPHOS subunits that were encoded by mtDNA and nuclear genes.

Results

Variations in the steady-state levels of mt-tRNAs among mouse-derived tissues

To investigate the tissue-specific expression of mt-tRNAs in mice, we subjected total RNAs from brain, heart, liver, skeletal muscle, and kidney to Northern blots and hybridized them with digoxigenin (DIG)-labeled oligodeoxynucleotide probes for 14 mt-tRNAs from H-strand transcripts and 8 mt-tRNAs from L-strand transcripts, cytosolic (ct) tRNA

(ct-tRNA^{Asp(GTC)}, ct-tRNA^{Lys(TTT)}, and ct-tRNA^{Lys(CTT)}) as well as with reference 5S rRNA, a nuclear-encoded mitochondrial small RNA (31, 32). For comparison, the average levels of each tRNA among different tissues were then normalized to the average levels in the 5S rRNA of the same tissue. As shown in Figure 1A and Table S1, there were marked differences in the levels of each mt-tRNA among the five tissues. For example, the average levels of tRNA^{His} among the brain, heart, liver, skeletal muscle, and kidney were 0.87, 2.34, 0.20, 0.75, and 0.84-fold relative to average levels of this tRNA among five tissues, respectively. As shown in Figure 1A, various differing levels of these 22 mt-tRNAs were observed in the same tissue type. As shown in the Figure 1B and Table S1, the average levels of mt-tRNAs ranged from 1.54-fold (tRNA^{Leu(UUR)}) to 2.34-fold (tRNA^{His}) (relative to average of corresponding tRNA among five tissues) in the heart, 0.61-fold

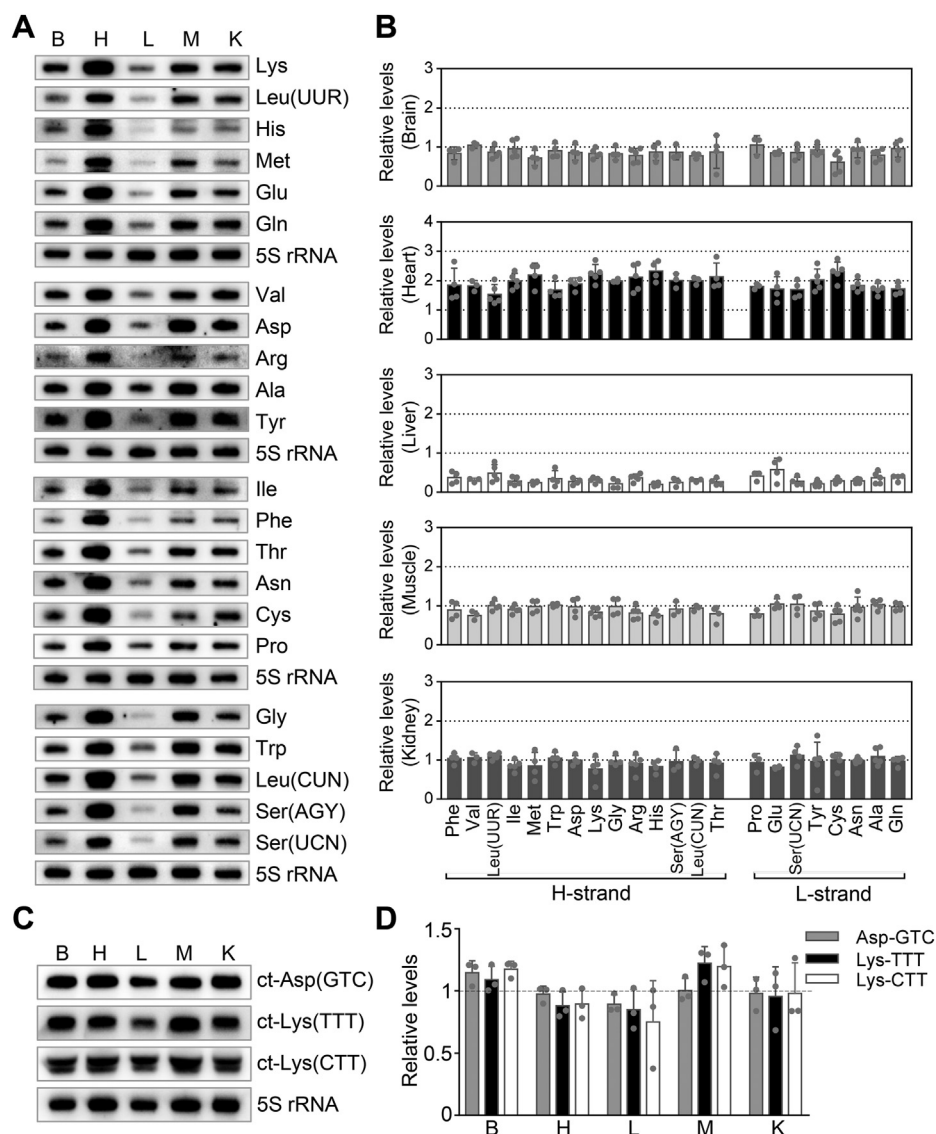


Figure 1. Northern blot analysis of 22 mt-tRNA steady-state levels among five mouse tissues. A and C, four micrograms of total RNA from mouse-derived brain, heart, liver, skeletal muscle, and kidney tissues was electrophoresed through a denaturing polyacrylamide gel, electroblotted, and hybridized with DIG-labeled oligonucleotide probes specific for the 22 mt-tRNAs, ct-tRNA^{Asp(GTC)}, tRNA^{Lys(TTT)} and tRNA^{Lys(CTT)} and 5S rRNA, respectively. B and D, quantification of relative mt-tRNA levels of the five tissues. The content of each mt-tRNA was normalized to that of 5S rRNA in the five tissues. Relative tRNA levels for the brain, heart, liver, skeletal muscle, and kidney were normalized to the mean values of each tRNA among the five tissues. Calculations were based on 3 to 5 independent experiments. Error bars indicate two standard deviations (SD) of the means. B, Brain; H, Heart; K, Kidney; L, liver; M, skeletal muscle.

(tRNA^{Cys}) to 1.05-fold (tRNA^{Val}, tRNA^{Pro}) in the brain, 0.75-fold (tRNA^{His}) to 1.04-fold (tRNA^{Glu}, tRNA^{Ser(UCN)}) in the skeletal muscle, 0.77-fold (tRNA^{Lys}) to 1.12-fold (tRNA^{Ser(UCN)}) in the kidney, and 0.20-fold (tRNA^{His}) to 0.58-fold (tRNA^{Glu}) in the liver. Strikingly, the heart exhibited the highest levels of average 22 mt-tRNAs (1.92-fold relative to average levels of 22 mt-tRNAs in five tissues). Brain, skeletal muscle, and kidney also revealed relatively higher levels of average 22 mt-tRNAs (0.86, 0.92, and 0.98 fold, respectively). The liver exhibited markedly lower levels of average 22 mt-tRNAs (0.31-fold relative to average levels of 22 mt-tRNAs in five tissues). However, there was no significant difference in the levels of ct-tRNA^{Asp(GTC)}, ct-tRNA^{Lys(TTT)}, and ct-tRNA^{Lys(CTT)} among the brain, heart, liver, skeletal muscle, and kidney tissues (Fig. 1, C and D). These variations in the levels of mt-tRNAs may reflect the mtDNA contents among these tissues. We measured relative mtDNA copy numbers from five mouse-derived tissues by comparing the ratios of mtDNA to nDNA by real-time quantitative PCR (33). As shown in Fig. S1A, there were marked variations in the mtDNA copy numbers among five tissues. Notably, the mtDNA contents of the brain, heart, skeletal muscle, kidney, and liver were 1.01, 1.66, 1.05, 0.66, and 0.63-fold, relative to the overall average levels of those in five tissues combined, respectively. As shown in Fig. S1B, the variations in the levels of mt-tRNAs in five tissues showed significant correlations with the corresponding variations in mtDNA copy numbers ($r^2 = 0.78$, $p = 0.048$). These results suggested that the differences of mitochondrial copy numbers contributed significantly to the variations of tRNA levels.

Thiolation levels of mitochondrial tRNA^{Lys}, tRNA^{Gln}, and tRNA^{Glu}

In the human mitochondrion, 18 types of nucleotide modification are present in the 137 positions of 22 mt-tRNA species (14). In particular, 5-taurinomethyl-2-thiouridine ($\text{rm}^5\text{s}^2\text{U}$) modification was only present in the tRNA^{Lys}, tRNA^{Glu}, and tRNA^{Gln} but not in other tRNAs (14). The presence of thiouridine modification in these tRNAs was examined using retardation of electrophoretic mobility in a polyacrylamide gel containing 0.05 mg/ml (*N*-acryloylaminophenyl) mercuric

chloride (APM) (29). In this study, the levels in the 2-thiouridine modification at position U34 in tRNA^{Lys}, tRNA^{Glu}, and tRNA^{Gln} were determined by isolating total RNAs from mouse brain, heart, liver, skeletal muscle, and kidney tissues, then purifying tRNAs, qualifying the 2-thiouridine modification by retardation of electrophoresis mobility in APM polyacrylamide gel (27–29), and hybridizing DIG-labeled probes for mitochondrial tRNA^{Gln}, tRNA^{Glu} and tRNA^{Lys} and tRNA^{Leu(UUR)}. In this system, the mercuric compound can specifically interact with the tRNAs containing a thiocarbonyl group such as tRNA^{Gln}, tRNA^{Glu}, and tRNA^{Lys}, thereby retarding tRNA migration. As shown in Figure 2, $\text{rm}^5\text{s}^2\text{U}$ levels of tRNA^{Lys} in the brain, heart, liver, skeletal muscle, and kidney tissues were 97.9%, 89.1%, 96.3%, 95.6%, and 96.6%, respectively; $\text{rm}^5\text{s}^2\text{U}$ levels of tRNA^{Glu} in the brain, heart, liver, skeletal muscle, and kidney were 78%, 72.4%, 72.6%, 76.1%, and 79.6%, respectively, and $\text{rm}^5\text{s}^2\text{U}$ levels of tRNA^{Gln} in the brain, heart, liver, skeletal muscle, and kidney were 87.8%, 83%, 82.6%, 85%, and 86.1%, respectively. However, $\text{rm}^5\text{s}^2\text{U}$ was absent in the mitochondrial tRNA^{Leu(UUR)}. No significant differences in the $\text{rm}^5\text{s}^2\text{U}$ levels of tRNA^{Lys}, tRNA^{Glu}, and tRNA^{Gln} were observed among these five tissues.

Aminoacylation levels of mitochondrial tRNAs

Aminoacylation is an essential step in the synthesis of proteins (17). We examined the aminoacylation levels of 15 mt-tRNAs including tRNA^{Met}, tRNA^{Leu(UUR)}, tRNA^{Leu(CUN)}, tRNA^{Ile}, tRNA^{His}, ct-tRNA^{Lys(TTT)}, and ct-tRNA^{Lys(CTT)} in the five tissues, by the use of electrophoresis in an acidic urea PAGE system to separate uncharged tRNA species from the corresponding charged tRNA, electroblotting and hybridizing with the tRNA probes described above (18). As shown in Figure 3 and Table S2, various aminoacylation levels of each tRNA were observed among the five tissues. There were marked differences of aminoacylation levels in these mt-tRNAs such as tRNA^{Leu(UUR)}, tRNA^{Leu(CUN)}, tRNA^{Gly}, tRNA^{Pro}, and tRNA^{Tyr} among five tissues. In particular, the average levels of tRNA^{Leu(UUR)} aminoacylation among the brain, heart, liver, skeletal muscle, and kidney were 35.6%, 59.4%, 63.7%, 72.7%, and 21.3%, respectively. As shown in Figure 3A and Table S2, the various aminoacylation levels of the 15 mt-tRNAs were observed in the same tissue. Specially, the average aminoacylation levels of 15 mt-tRNAs varied from 15.2% in tRNA^{Pro} to

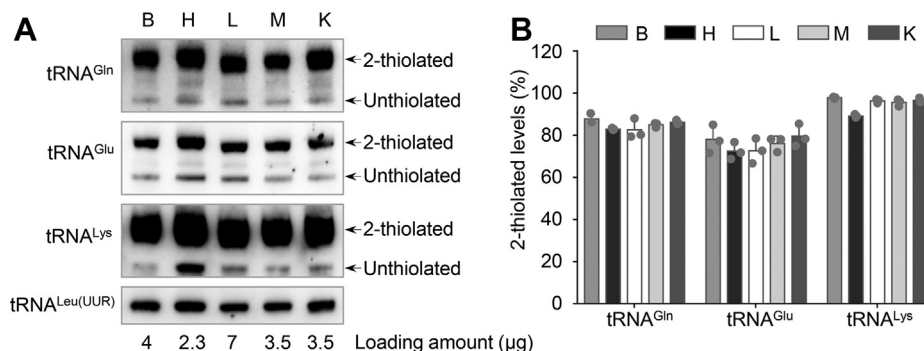


Figure 2. APM gel electrophoresis combined with Northern blot analysis of mt-tRNAs. A, four, 2.3, 7, 3.5, and 3.4 μg of total RNAs from the brain, heart, liver, skeletal muscle, and kidney tissues were separated by polyacrylamide gel electrophoresis containing 0.05 mg/ml APM, electroblotted onto a positively charged membrane, and hybridized with a DIG-labeled oligonucleotide probe specific for mt-tRNA^{Gln}, tRNA^{Glu}, tRNA^{Lys}, and tRNA^{Leu(UUR)}, respectively. B, quantification of 2-thiolated tRNA levels. Calculations were based on more than three independent experiments. Error bars indicate SD of the means.

Tissue-specific expression of murine mitochondrial tRNA

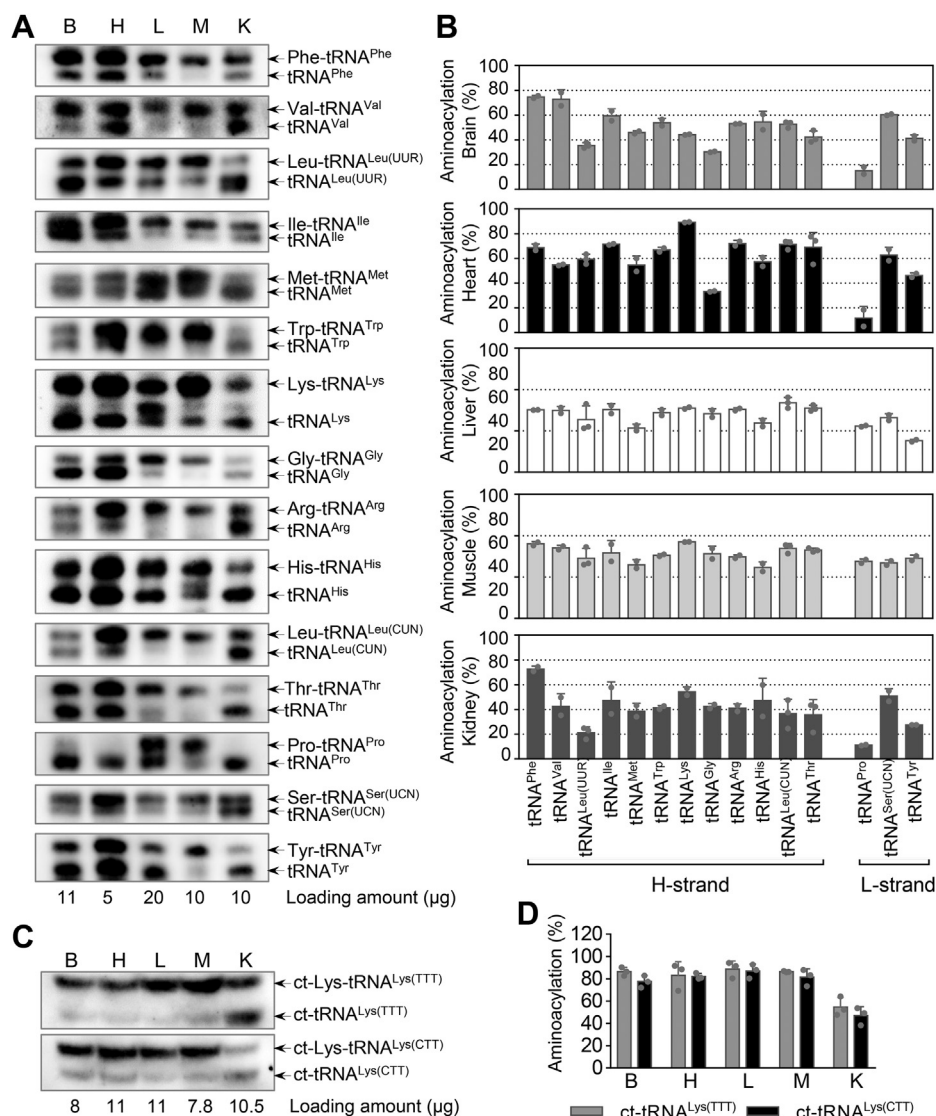


Figure 3. Aminoacylation analysis of tRNAs. A, Eleven, 5, 20, 10, or 10 μ g and C, 8, 11, 11, 7.8, or 10.5 μ g of total RNAs from mouse-derived brain, heart, liver, skeletal muscle, and kidney tissues, respectively, were electrophoresed at 4 $^{\circ}$ C through an acid (pH 5.0) 8.5% polyacrylamide with 8 M urea gel, electroblotted, and hybridized with a DIG-labeled oligonucleotide probes-specific for 15 mt-tRNAs and two ct-tRNAs. The charged (*upper band*) and uncharged (*lower band*) forms of different mt-tRNAs were separated by the gel system. B and D, quantification of aminoacylated proportions of tRNAs. Calculations were based on 2 to 3 independent determinations. Error bars indicate SD of the means.

74.6% in tRNA^{Phe} with an average 51% of 15 tRNAs in the brain, 11.7% in tRNA^{Pro} to 89.3% in tRNA^{Lys} with average 59.3% of 15 tRNAs in the heart, 38.1% in tRNA^{Tyr} to 84.1% in tRNA^{Leu(CUN)} with average 69.1% of 15 tRNA in the liver, 61.5% in tRNA^{His} to 92.5% in tRNA^{Lys} with average 77.9% of 15 tRNAs in the skeletal muscle, and 11.2% in tRNA^{Pro} to 72.6% in tRNA^{Phe} with average 40.3% of 15 mt-tRNAs in the kidney. As shown in Figure 3, C and D, there were no significant differences in aminoacylation levels of ct-tRNA^{Lys(TTT)} and ct-tRNA^{Lys(CTT)} among the brain, heart, liver, and skeletal muscle. However, there were relatively higher aminoacylation levels of cytosolic ct-tRNA^{Lys(TTT)} and ct-tRNA^{Lys(CTT)} in the kidney tissues.

Negative correlation between mt-aARS expression and tRNA aminoacylation

A specific cognate amino acid is charged or aminoacylated to each tRNA catalyzed by mt-aARSs (17). We measured the

mRNA expression levels of 14 genes encoding mt-aARSs among the five tissues using quantitative PCR for these genes and 18S rRNA as normalization. The average mRNA level of each gene in various tissues was then normalized to the average levels in the same tissue for the reference 18S rRNA. As shown in Figure 4A and Table S3, there were marked differences in the mRNA levels of each genes among the five tissues. For example, the average mRNA levels of *Fars2* among the brain, heart, liver, skeletal muscle, and kidney were 0.62, 1.56, 0.59, 0.53, and 1.7-fold relative to average mRNA levels of 15 genes in five tissues, respectively. As shown in Figure 4A and Table S3, the varied mRNA levels of these 15 genes were observed in the same tissue, with the average mRNA levels of the 15 genes ranging from 0.62-fold (*Fars2*) to 2.05-fold (*Mars2*) (relative to average of 15 genes among five tissues) in the brain, 0.74-fold (*Rars2*) to 1.56-fold (*Fars2*) in the heart, 0.24-fold (*Mars2*) to 0.68-fold (*Yars2*) in the liver, 0.45-fold

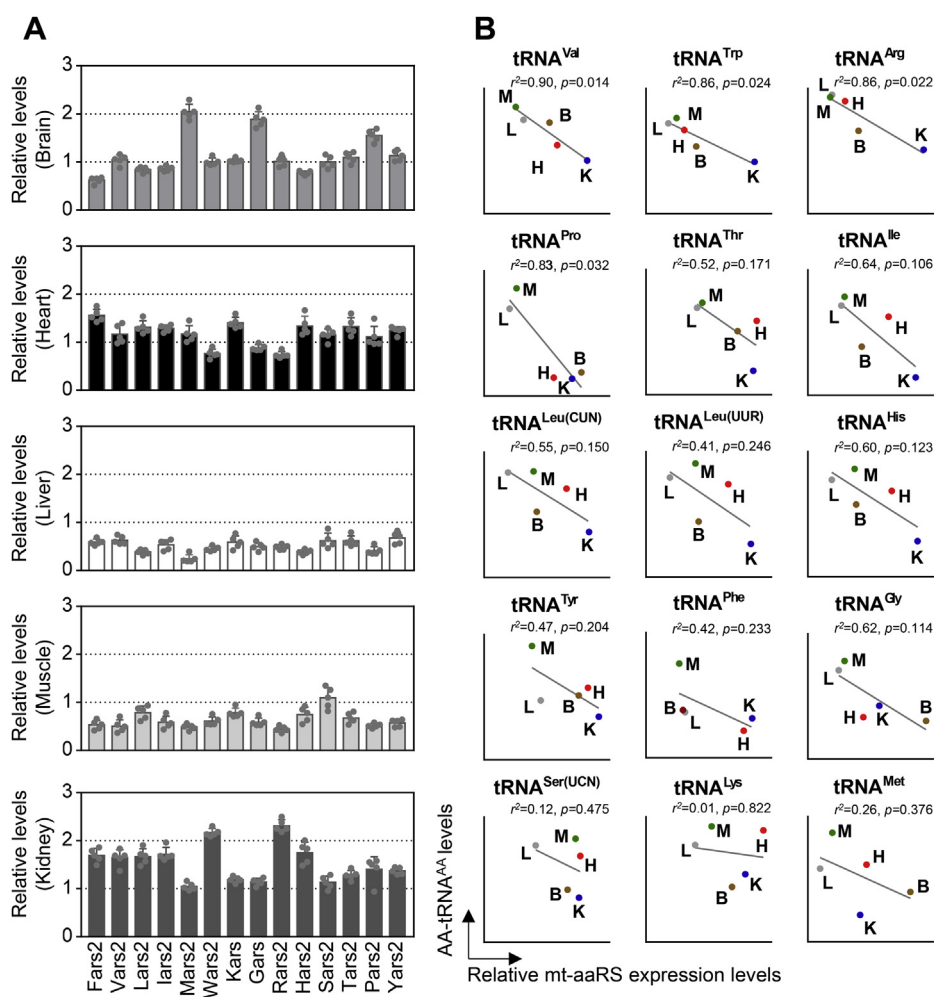


Figure 4. Mt-aaRS gene expression analysis. A, the relative expression levels of mt-aaRS genes from mouse-derived brain, heart, liver, skeletal muscle, and kidney tissues using RT-qPCR. Relative levels were normalized to the mean values of each mt-aaRS gene among five tissues. n=5 per group. B, Pearson correlation was used to measure the extent of correlation between the mean level of mt-aaRS expression and corresponding mt-tRNA aminoacylation in each of the five tissues. The r^2 and p values are indicated in each graph.

(*Rars2*) to 1.1-fold (*Sars2*) in the skeletal muscle, and 1.05-fold (*Mars2*) to 2.31-fold (*Rars2*) in the kidney.

We then investigated if there was any potential correlation between the mt-aaRS mRNA levels and mt-tRNA aminoacylation levels in various tissues. As shown in Figure 4B, the variations in the aminoacylation levels in the mt-tRNAs among the five tissues exhibited negative correlations with the corresponding variations in the aaRS mRNA levels. In particular, the aminoacylation levels in the tRNA^{Val}, tRNA^{Trp}, tRNA^{Arg}, and tRNA^{Pro} revealed significantly negative correlation with the corresponding variations in aaRS expression levels in these five tissues ($r^2 = 0.90, p = 0.014$; $r^2 = 0.86, p = 0.024$; $r^2 = 0.86, p = 0.022$; $r^2 = 0.83, p = 0.032$, respectively). However, the correlations between aminoacylation levels of other ten tRNAs and mRNA levels of their corresponding aaRS were not statistically significant.

Tissue-specific expression of OXPHOS subunits

To assess the tissue-specific expression of OXPHOS subunits, we examined the levels of the subunits of OXPHOS in the five tissues using western blot analysis. These subunits

included six mtDNA encoding polypeptides (Nd1, Nd3, Co1, Co2, Atp6, and Atp8), seven nucleus encoding proteins: Ndufa9 and Ndufb8 [subunits of NADH dehydrogenase (complex I)], Sdha and Sdhb [subunits of succinate dehydrogenase (complex II)], Uqcrc2 [subunit of ubiquinol-cytochrome c reductase (complex III)], Cox4 (subunit of complex IV), and Atp5a [subunit of H⁺-ATPase (complex V)] (3). As shown in Figure 5 and Table S4, there were varying levels of each subunit among the five tissues. Co1, Co2, Cox4, subunits of complex IV exhibited marked differences in the levels of these proteins among the five tissues, especially extremely high expression in the heart. The Nd1, Nd3, Ndufa9, and Ndufb8 subunits of complex I revealed relatively low variations in the levels of these proteins among these five tissues. As shown in Figure 5 and Table S4, the average levels of 13 subunits ranged from 0.41-fold (Co2) to 1.15-folds (Atp6) with average of 0.73-fold (relative to average of 13 subunits among five tissues) in the brain, 1.2-fold (Nd1) to 3.21-fold (Co1) with average of 1.99 fold in the heart, 0.09-fold (Cox4) to 0.73-fold (Sdhb) with the average of 0.49-fold in the liver, 0.57-fold (Co1) to 1.13-fold (Ndufb8) with average of 0.92-fold

Tissue-specific expression of murine mitochondrial tRNA

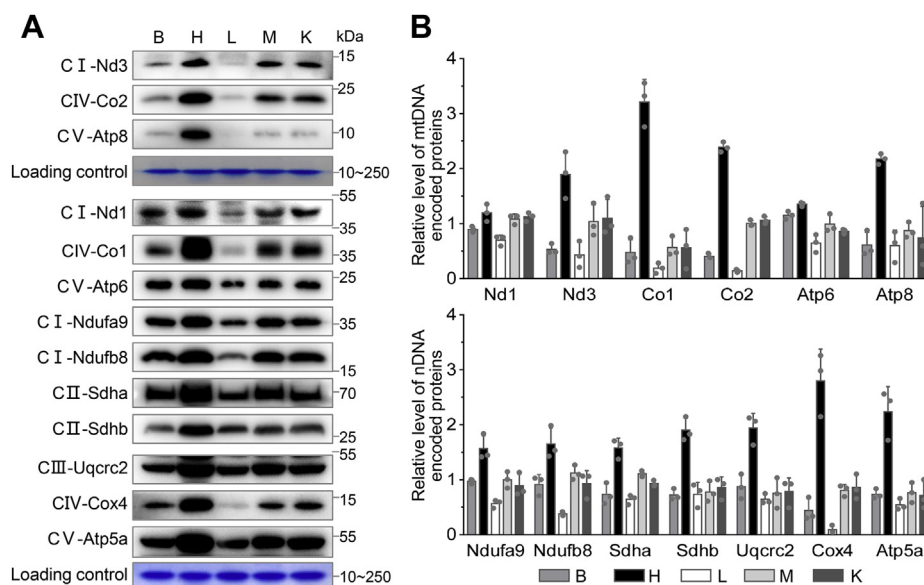


Figure 5. Western blotting analysis of mitochondrial proteins. A, eight micrograms of total cellular proteins from five mouse-derived tissue types was electrophoresed through a denaturing polyacrylamide gel, electroblotted, and corresponding Coomassie Brilliant Blue stained gel were used as loading control. The blots were hybridized with antibodies for 11 subunits of OXPHOS (six encoded by mtDNA and seven encoded by nDNA). B, quantification of OXPHOS subunits levels in the five tissues. The content of each proteins was normalized to that of total cellular protein in the five tissues. Relative protein levels for the brain, heart, liver, skeletal muscle, and kidney tissues were normalized to the mean values of each protein among the five tissues. Calculations were based on three independent determinations. Error bars indicate SD of the means.

in the skeletal muscle, and 0.56-fold (Co1) to 1.12-fold (Nd1) with average of 0.88-fold in the kidney. Notably, the variations in the average levels of mtDNA encoding proteins among five tissues showed significant correlations with the corresponding variations in mtDNA copy numbers ($r^2 = 0.81$, $p = 0.039$) or with mt-tRNA levels ($r^2 = 0.95$, $p = 0.048$) (Fig. S1, C and D). These data suggested that the mtDNA contents and mt-tRNA levels may reflect the tissue-specific expressions of OXPHOS subunits.

Discussion

Mammalian tissues differ in many aspects in their metabolic profiles and energy demands during development, physiological adaptation, and pathology. In mammalian cell, mitochondria produce energy through the process of oxidative phosphorylation, and the extent of their occurrence in tissues varies depending on age, organ, and/or physiological condition (34). The copy number of mtDNA reflects the abundance of mitochondria within a cell and is regulated by transcriptional and translational factors (33–35). Essential for the synthesis of essential subunits of OXPHOS, mt-tRNAs play central roles in cellular functions in health and disease. However, the tissue-specific expression and physiological conditions of mammalian mt-tRNAs and the mechanisms underlying tissue-specific effects of the mt-tRNA mutations linked to clinical presentations are largely unknown. In this study, we demonstrated the striking differences in the tissue-specific expression of 22 mt-tRNAs in mouse-derived brain, heart, liver, skeletal muscle, and kidney tissues. In particular, the heart exhibited the highest levels of average 22 mt-tRNAs, the brain, skeletal muscle, and kidney revealed relatively higher levels of average 22 mt-tRNAs, and the liver exhibited markedly lower levels of

average 22 mt-tRNAs. These variations in the levels of mt-tRNAs may reflect the mtDNA contents among these tissues, as the mtDNA contents of the heart were much higher than those in the brain, liver, skeletal muscle, and kidney (33). In particular, the variations in the levels of mt-tRNAs in the five tissues showed a significant correlation with the corresponding variations in mtDNA copy numbers. These results suggested that the differences of mtDNA copy number contributed to the variations of tRNA levels among these five tissues. Alternatively, these wide variations of tRNA abundances suggested that tRNAs may be dynamically related to specific activities, not just to general accumulation levels among these tissues. The tRNA, with traditional functions in translation, plays a role in the tissue-specific post-transcriptional regulations and translational heterogeneity *via* availability of certain tRNAs (20, 36). By contrast, the relatively mild differences in those cytosolic tRNAs (ct-tRNA^{Lys(TTT)}, ct-tRNA^{Lys(CTT)}, and ct-tRNA^{Asp(GTC)}) among these tissues were comparable with those of previous studies (19).

There were 18 types of nucleotide modifications present in the 137 positions of human 22 mt-tRNAs (14). These nucleotide modifications included pseudouridine (Ψ) at position 55 at the TYC loop, nucleotides at positions 34 and 37 at the anticodon loop of tRNAs (4, 14, 37). Posttranscriptional modifications of tRNAs affect all aspects of tRNA structure and function (38). Using APM gel, we focused on the analysis of the levels of 2-thiouridine modification at position 34 in mitochondrial tRNA^{Lys}, tRNA^{Gln}, and tRNA^{Glu} among five mouse-derived tissues. There were no significant differences in the $\text{m}^5\text{s}^2\text{U}$ levels of tRNA^{Lys}, tRNA^{Glu}, and tRNA^{Gln} among these five tissues. These suggested that there may be no tissue-specific $\text{m}^5\text{s}^2\text{U}$ modifications of tRNAs among these tissues,

in contrast with the marked variations in the steady-state levels of tRNAs among the mouse organs represented, as described above.

Aminoacylation, the attachment of an amino acid to an mt-tRNA, is catalyzed by mitochondrial aminoacyl-tRNA synthetases (4, 30). During protein synthesis, charged mt-tRNAs deliver amino acids to translating ribosomes and are then recharged by tRNA synthetases. Notably, the *Wars2* and *Dars2* mutant mice displayed tissue-specific effects of mitochondrial deficiencies (22, 39). In this study, we examined the aminoacylation levels of 15 mt-tRNAs including tRNA^{Met}, tRNA^{Leu(UUR)}, tRNA^{Leu(CUN)}, tRNA^{Ile}, and tRNA^{His} among the five mouse-derived tissues. We demonstrated wide ranges in aminoacylation levels between each mt-tRNA type among these five tissues and of these 15 tRNAs in the same tissue. In fact, 15 tRNAs including tRNA^{Leu(UUR)}, tRNA^{Leu(CUN)}, tRNA^{Gly}, tRNA^{Pro}, and tRNA^{Tyr} displayed striking differences in aminoacylation levels among these tissues. In particular, the average aminoacylation levels of tRNA^{Pro} among the brain, heart, liver, skeletal muscle, and kidney were 15.2%, 11.7%, 55.8%, 68.9%, and 11.2%, respectively. In contrast, tRNA^{His}, tRNA^{Thr}, and tRNA^{Phe} revealed relatively low discrepancies of aminoacylation levels among these tissues. Especially, the average aminoacylation levels of tRNA^{Thr} among the brain, heart, liver, skeletal muscle, and kidney were 60.3%, 62.8%, 65.9%, 67.1%, and 50.8%, respectively. Furthermore, the overall average aminoacylation levels of the 15 mt-tRNAs in the brain, heart, liver, skeletal muscle, and kidney were 51%, 59.3%, 69.1%, 77.9%, and 40.3%, respectively. However, such variations in aminoacylation levels of the 15 mt-tRNAs were not significantly correlated with the steady-state levels of these tRNAs among five tissues and may instead reflect the translation efficiencies for the heterogeneity of protein synthesis among tissues. Furthermore, we measured the mRNA expression levels of the 14 mt-aaRSs encoding genes among the five tissues. Marked differences in the levels of each gene were observed among the five tissues, the average expression levels of these genes among the brain, heart, liver, skeletal muscle, and kidney being 1.14, 1.18, 0.51, 0.64, and 1.54-fold, respectively, relative to average levels of these five tissues combined. Remarkably, the variations in the aminoacylation levels of mt-tRNAs among the five tissues exhibited negative correlations with the corresponding variations in their mt-aaRS expression levels. These may be due to a negative feedback mechanism that matches translational demand for aminoacylated mt-tRNA to the aaRS recharging capacity (40). In fact, a reduced abundance of mt-aaRS could interfere with the normal ability of the synthetase to sequester the uncharged tRNA pool. Alternatively, T-box riboswitches in mitochondria may regulate the expression of aminoacyl-tRNA synthetases and other proteins in response to fluctuating transfer RNA aminoacylation levels under various nutritional or physiological states (41).

Thirteen polypeptides synthesized by mitochondrial translations were the essential subunits of OXPHOS machinery, while other 77 OXPHOS subunits were encoded by nuclear genes and synthesized in cytosol and then imported into mitochondria (3). The specific oxidative phosphorylation capacities of cells or tissues depend on their metabolic and energetic demands (42, 43). To assess the tissue-specific impacts

of mitochondrial tRNA metabolism on translation and OXPHOS biogenesis across tissues, we examined the levels of six mtDNA encoding OXPHOS subunits (Nd1, Nd3, Co1, Co2, Atp6, and Atp8) and seven nucleus encoding OXPHOS subunits (Ndufa9, Ndubf8, Sdha, Sdhb, Uqcrc2, Cox4, and Atp5a), noting the various levels of these 13 proteins according to tissue type. All of these OXPHOS subunits were expressed at much higher levels in the heart than in any other tissues. The average levels of 13 OXPHOS subunits ranged from 0.73-fold in the brain, 2.04-fold in the heart, 0.47-fold in the liver, 0.9-fold in the skeletal muscle, and 0.86-fold in the kidney. Furthermore, we revealed the various levels of each subunit among the five tissues. The Co1, Co2, and Cox4 subunits of complexes IV exhibited marked differences in the levels of these proteins among the five tissues, with especially high expressions in the heart. Conversely, the Nd1, Nd3, Ndufa9, and Ndubf8 subunits of complex I revealed relatively low variations in the levels of these proteins among these five tissues. Notably, the variations in levels of these proteins were significantly correlated with the steady levels of mitochondrial tRNAs ($r^2 = 0.9498$, $p = 0.0048$) but not with the aminoacylation levels of these tRNAs among these tissues. These various expressions of these OXPHOS subunits may reflect the relative functional emphasis of mitochondria among different tissues (44). Mitochondria in the brain are specialized to the neurotransmitter metabolism, while in the heart mitochondria are specialized for constant and effective production of ATP by the means of β -oxidation (45). These are also inherently different from mitochondria in the liver and kidney, which are more specialized for the various reactions of anabolic and catabolic metabolism (45). Therefore, the tissue-specific metabolic aspects of mitochondrial tRNA and related expression levels of these OXPHOS subunits are accounted for by these tissue-specific requirements and facilitated by their specialized mitochondrial features in different tissues.

In summary, we demonstrated the tissue-specific metabolisms of 22 mt-tRNAs. We showed that the steady-state levels of 22 tRNAs varied as much as tenfold among these tissues. The heart, in particular, exhibited the highest levels of tRNAs. There were no significant differences in the 2-thiouridylation levels of tRNA^{Lys}, tRNA^{Glu}, and tRNA^{Gln} among these tissues. We demonstrated a wide range of aminoacylation levels of each tRNA among these tissues, with skeletal muscle revealing the highest aminoacylation levels of tRNAs. Aminoacylation levels of mt-tRNAs exhibited negative correlations with the variations in mitochondrial tRNA synthetase expressions among these tissues, while the variations of tRNA abundances were significantly correlated with the levels of OXPHOS subunits. Our findings may provide new insights into the mechanism of mt-tRNA tissue-specific effects on physiological conditions.

Experimental procedures

Mice

All animal care protocols were approved by the Animal Care and Use Committee of Zhejiang University. C57BL/6 mice

Tissue-specific expression of murine mitochondrial tRNA

were purchased from Shanghai Slac Animal Inc. Mice were housed in a 12-h light/dark cycle and provided food and water *ad libitum* in the Experimental Animal Center of Zhejiang University. The 8~12-week-old male or virgin female mice were sacrificed by cervical dislocation. For liver samples, only the largest lobe of the mouse liver was used. Whole organs were then dissected in the following order: brain, heart, kidney, and skeletal muscle (tibialis anterior).

Mitochondrial tRNA analysis

Total RNAs from various mice tissues were obtained by using TOTALLY RNA kit (Ambion), as detailed elsewhere (46). For tRNA Northern blot analysis, 4 μ g of total RNAs was electrophoresed through a 10% polyacrylamide/8 M urea gel in 1 \times TBE buffer after heating the samples at 95 °C for 5 min and then electroblotted onto a positively charged nylon membrane (Millipore) for hybridization analysis with the respective DIG-labeled oligodeoxynucleotide probes. The set of DIG-labeled probes of 22 mt-tRNAs, 5S rRNA, and ct-tRNA^{Lys(TTT)}, tRNA^{Lys(CTT)}, and tRNA^{Asp(GTC)} used for this study were listed in the Table S5 (47). The specificities of these tRNA probes were analyzed using nucleotide BLAST (www.ncbi.nlm.nih.gov/BLAST/). The hybridization and quantification of density for each band were performed as detailed previously (25, 48).

The aminoacylation assays were carried out as detailed previously (18, 25). To further distinguish nonaminoacylated tRNA from aminoacylated tRNA, total RNAs were heated for 10 min at 60 °C at pH 9.0 and then run in parallel (18, 25). DIG-labeled oligodeoxynucleotide probes for mt-tRNAs and ct-tRNAs were as described above. The quantification for density in each band was performed as detailed previously (18, 25).

Thiouridine modification in the tRNAs was analyzed using the retardation of electrophoretic mobility in a polyacrylamide gel containing 0.05 mg/ml APM (27–29). Total RNAs were separated using polyacrylamide gel electrophoresis and blotted onto positively charged membrane (Roche Applied Science). Each tRNA was detected with the specific DIG-oligodeoxynucleoside probe at the 3' termini as detailed elsewhere (29, 49). Oligonucleotide probes for mitochondrial tRNA^{Lys}, tRNA^{Glu}, tRNA^{Gln}, and tRNA^{Leu(UUR)} were described as above. DIG-labeled oligodeoxynucleosides were generated by using the DIG Oligonucleoside Tailing Kit (Roche). APM gel electrophoresis and quantification of 2-thiouridine modification in tRNAs were conducted as detailed (27, 49).

Western blotting analysis

Western blotting analysis was performed as detailed previously (9, 25, 50). Twenty micrograms of total cell proteins obtained from each of the various tissues was denatured and loaded on sodium dodecyl sulfate (SDS) polyacrylamide gels. The gels were electroblotted onto a polyvinylidene difluoride (PVDF) membrane for hybridization. The antibodies obtained from different companies were as follows: Abcam [Nd1 (ab74257), Co1 (ab14705), Co2 (ab198286), Ndufb8 (ab110242), Ndufa9 (ab14713), Sdhd (ab14714), Uqcrc2 (ab14745), and Atp5a (ab14748)], Diageno [Cox4 (db15)] and

Proteintech [Atp6 (55313-1-AP), Atp8 (26723-1-AP), and Sdha (14865-1-AP)]. Peroxidase Affini Pure goat anti-mouse IgG and goat anti-rabbit IgG (Jackson) were used as secondary antibodies and protein signals were detected using the ECL system (CWBI). Quantification of the density of each band was performed as detailed previously (9, 25, 49, 50).

Measurement of mtDNA/nDNA

Total DNA was isolated from each of the various mouse tissues using a Tissue gDNA kit (Biomiga) according to the manufacturer's protocol. Primers for mouse mtDNA (Mito) and mouse nDNA (B2M) were used to amplify the respective products from mouse genomic DNA (Table S6). MtDNA content was determined by comparing the ratio of mtDNA to nDNA by real-time quantitative PCR (33). The relative ratio was analyzed on a 7900HT system (Applied Biosystems) using FastStart Universal SYBR Green Master Mix (Roche Diagnostics GmbH).

Gene expression analysis of 14 genes encoding mt-aaRSs

Total RNA was extracted from each of the various mouse using TRIzol reagent (Ambion) and reverse transcribed into cDNA using PrimeScript II first Strand cDNA Synthesis Kit (Takara). Quantitative PCR was performed on the Applied Biosystems 7900HT Fast Real-Time PCR System. Data were analyzed using the 7900 System SDS RQ Manager Software, and the gene expression levels of the 14 genes encoding mt-aaRSs were determined using the $2^{-\Delta\Delta C_t}$ method using nucleus encoded 18S rRNA as normalization. Primer sequences for this analysis were listed in Table S6.

Statistical analysis

All statistical analysis was performed using unpaired, two-tailed Student's *t* test contained in the Graphpad prism 8 program (Graphpad software) and Microsoft-Excel program (version 2016). A *p* value <0.05 was considered statistically significant.

Data availability

Representative experiments are shown in the figures and supplemental materials. For any additional information, please contact the corresponding author.

Supporting information—This article contains [supporting information](#).

Author contributions—M.-X. G. and Y. C. conceptualization; Q. H., X. H., Y. X., Q. Z., Z. Y., L. C., and M.-X. G. data curation; Q. H. formal analysis; M.-X. G. funding acquisition; Q. H., X. H., and M.-X. G. investigation; Q. H., X. H., and Y. X. methodology; M.-X. G. project administration; M.-X. G. resources; Y. C. and M.-X. G. supervision; Q. H. and Q. Z. validation; Q. H. and Y. C. writing-original draft; M.-X. G. writing-review and editing.

Funding and additional information—This research was supported by grants from Grant 2018C03026 from Ministry of Science and

Technology of Zhejiang Province, the National Key Technologies R&D Program Grant 2018YFC1004802 from the Ministry of Science and Technology of China (to M.-X. G.), 82030028 (M.-X. G.), and 31671305 (Y. C.) from the National Natural Science Foundation of China.

Conflict of interest—All authors declare that they have no conflict of interest with contents of this article.

Abbreviations—The abbreviations used are: DIG, digoxigenin; mRNA, messenger RNA; mt-aaRS, mitochondrial tRNA synthetases; mt-tRNA, mitochondrial tRNA; mtDNA, mitochondrial DNA; OXPHOS, oxidative phosphorylation complex system.

References

- Anderson, S., Bankier, A. T., Barrell, B. G., de Bruijn, M. H., Coulson, A. R., Drouin, J., Eperon, I. C., Nierlich, D. P., Roe, B. A., Sanger, F., Schreier, P. H., Smith, A. J., Staden, R., and Young, I. G. (1981) Sequence and organization of the human mitochondrial genome. *Nature* **290**, 457–465
- Bibb, M. J., Van Etten, R. A., Wright, C. T., Walberg, M. W., and Clayton, D. A. (1981) Sequence and gene organization of mouse mitochondrial DNA. *Cell* **26**, 167–180
- Wallace, D. C. (2013) A mitochondrial bioenergetic etiology of disease. *J. Clin. Invest.* **123**, 1405–1412
- Suzuki, T., Nagao, A., and Suzuki, T. (2011) Human mitochondrial tRNAs: Biogenesis, function, structural aspects, and diseases. *Annu. Rev. Genet.* **45**, 299–329
- Montoya, J., Gaines, G. L., and Attardi, G. (1983) The pattern of transcription of the human mitochondrial rRNA genes reveals two overlapping transcription units. *Cell* **34**, 151–159
- Ojala, D., Montoya, J., and Attardi, G. (1981) tRNA punctuation model of RNA processing in human mitochondria. *Nature* **290**, 470–474
- Mercer, T. R., Neph, S., Dinger, M. E., Crawford, J., Smith, M. A., Shearwood, A. M., Haugen, E., Bracken, C. P., Rackham, O., Stamatoyannopoulos, J. A., Filipovska, A., and Mattick, J. S. (2011) The human mitochondrial transcriptome. *Cell* **146**, 645–658
- Scarpulla, R. C. (2008) Transcriptional paradigms in mammalian mitochondrial biogenesis and function. *Physiol. Rev.* **88**, 611–638
- Xiao, Y., Wang, M., He, Q., Xu, L., Zhang, Q., Meng, F., Jia, Z., Zhang, F., Wang, H., and Guan, M. X. (2020) Asymmetrical effects of deafness-associated mitochondrial DNA 7516delA mutation on the processing of RNAs in the H-strand and L-strand polycistronic transcripts. *Nucleic Acids Res.* **48**, 11113–11129
- Zhao, X., Cui, L., Xiao, Y., Mao, Q., Aishanjiang, M., Kong, W., Liu, Y., Chen, H., Hong, F., Jia, Z., Wang, M., Jiang, P., and Guan, M. X. (2019) Hypertension-associated mitochondrial DNA 4401A>G mutation caused the aberrant processing of tRNA^{Met}, all 8 tRNAs and ND6 mRNA in the light-strand transcript. *Nucleic Acids Res.* **47**, 10340–10356
- Sanchez, M. I., Mercer, T. R., Davies, S. M., Shearwood, A. M., Nygard, K. K., Richman, T. R., Mattick, J. S., Rackham, O., and Filipovska, A. (2011) RNA processing in human mitochondria. *Cell Cycle* **10**, 2904–2916
- Brzeznick, L. K., Bijata, M., Szczesny, R. J., and Stepien, P. P. (2011) Involvement of human ELAC2 gene product in 3' end processing of mitochondrial tRNAs. *RNA Biol.* **8**, 616–626
- Holzmann, J., Frank, P., Löffler, E., Bennett, K. L., Gerner, C., and Rossmanith, W. (2008) RNase P without RNA: Identification and functional reconstitution of the human mitochondrial tRNA processing enzyme. *Cell* **135**, 462–474
- Suzuki, T., Yashiro, Y., Kikuchi, I., Ishigami, Y., Saito, H., Matsuzawa, I., Okada, S., Mito, M., Iwasaki, S., Ma, D., Zhao, X., Asano, K., Lin, H., Kirino, Y., Sakaguchi, Y., et al. (2020) Complete chemical structures of human mitochondrial tRNAs. *Nat. Commun.* **11**, 4269
- Meng, F., Zhou, M., Xiao, Y., Mao, X., Zheng, J., Lin, J., Lin, T., Ye, Z., Cang, X., Fu, Y., Wang, M., and Guan, M. X. (2021) A deafness-associated tRNA mutation caused pleiotropic effects on the m¹G37 modification, processing, stability and aminoacylation of tRNA^{Leu} and mitochondrial translation. *Nucleic Acids Res.* **49**, 1075–1093
- Hou, Y. M. (2010) CCA addition to tRNA: Implications for tRNA quality control. *IUBMB Life* **62**, 251–260
- Sissler, M., González-Serrano, L. E., and Westhof, E. (2017) Recent advances in mitochondrial aminoacyl-tRNA synthetases and disease. *Trends Mol. Med.* **23**, 693–708
- Enriquez, J. A., and Attardi, G. (1996) Analysis of aminoacylation of human mitochondrial tRNAs. *Methods Enzymol.* **264**, 183–196
- Torres, A. G., Reina, O., Stephan-Otto Attolini, C., and Ribas de Pouplana, L. (2019) Differential expression of human tRNA genes drives the abundance of tRNA-derived fragments. *Proc. Natl. Acad. Sci. U. S. A.* **116**, 8451–8456
- Dittmar, K. A., Goodenbour, J. M., and Pan, T. (2006) Tissue-specific differences in human transfer RNA expression. *PLoS Genet.* **2**, e221
- Lant, J. T., Berg, M. D., Heinemann, I. U., Brandl, C. J., and O'Donoghue, P. (2019) Pathways to disease from natural variations in human cytoplasmic tRNAs. *J. Biol. Chem.* **294**, 5294–5308
- Agnew, T., Goldsworthy, M., Aguilar, C., Morgan, A., Simon, M., Hilton, H., Esapa, C., Wu, Y., Cater, H., Bentley, L., Scudamore, C., Poulton, J., Morten, K. J., Thompson, K., He, L., et al. (2018) A Wars2 mutant mouse model displays OXPHOS deficiencies and activation of tissue-specific stress response pathways. *Cell Rep.* **25**, 3315–3328
- Huttlin, E. L., Jedrychowski, M. P., Elias, J. E., Goswami, T., Rad, R., Beausoleil, S. A., Villén, J., Haas, W., Sowa, M. E., and Gygi, S. P. (2010) A tissue-specific atlas of mouse protein phosphorylation and expression. *Cell* **143**, 1174–1189
- Kirchner, S., and Ignatova, Z. (2015) Emerging roles of tRNA in adaptive translation, signalling dynamics and disease. *Nat. Rev. Genet.* **16**, 98–112
- Zhou, M., Xue, L., Chen, Y., Li, H., He, Q., Wang, B., Meng, F., Wang, M., and Guan, M. X. (2018) A hypertension-associated mitochondrial DNA mutation introduces an m¹G37 modification into tRNA^{Met}, altering its structure and function. *J. Biol. Chem.* **293**, 1425–1438
- Wang, M., Peng, Y., Zheng, J., Zheng, B., Jin, X., Liu, H., Wang, Y., Tang, X., Huang, T., Jiang, P., and Guan, M. X. (2016) A deafness-associated tRNA^{Asp} mutation alters the m¹G37 modification, aminoacylation and stability of tRNA^{Asp} and mitochondrial function. *Nucleic Acids Res.* **44**, 10974–10985
- Meng, F., Cang, X., Peng, Y., Li, R., Zhang, Z., Li, F., Fan, Q., Guan, A. S., Fischel-Ghosian, N., Zhao, X., and Guan, M. X. (2017) Biochemical evidence for a nuclear modifier allele (A10S) in TRMU (methyl-aminomethyl-2-thiouridylate-methyltransferase) related to mitochondrial tRNA modification in the phenotypic manifestation of deafness-associated 12S rRNA mutation. *J. Biol. Chem.* **292**, 2881–2892
- Zhang, Q., Zhang, L., Chen, D., He, X., Yao, S., Zhang, Z., Chen, Y., and Guan, M. X. (2018) Deletion of Mtu1 (Trmu) in zebrafish revealed the essential role of tRNA modification in mitochondrial biogenesis and hearing function. *Nucleic Acids Res.* **46**, 10930–10945
- Umeda, N., Suzuki, T., Yukawa, M., Ohya, Y., Shindo, H., Watanabe, K., and Suzuki, T. (2005) Mitochondria-specific RNA-modifying enzymes responsible for the biosynthesis of the wobble base in mitochondrial tRNAs. Implications for the molecular pathogenesis of human mitochondrial diseases. *J. Biol. Chem.* **280**, 1613–1624
- Enriquez, J. A., Chomyn, A., and Attardi, G. (1995) MtDNA mutation in MERRF syndrome causes defective aminoacylation of tRNA^{Leu} and premature translation termination. *Nat. Genet.* **10**, 47–55
- Magalhaes, P. J., Andreu, A. L., and Schon, E. A. (1998) Evidence for the presence of 5S rRNA in mammalian mitochondria. *Mol. Biol. Cell* **9**, 2375–2382
- Jühling, F., Mörl, M., Hartmann, R. K., Sprinzl, M., Stadler, P. F., and Pütz, J. (2009) tRNAdb 2009: Compilation of tRNA sequences and tRNA genes. *Nucleic Acids Res.* **37**, D159–162
- Masuyama, M., Iida, R., Takatsuka, H., Yasuda, T., and Matsuki, T. (2005) Quantitative change in mitochondrial DNA content in various mouse tissues during aging. *Biochim. Biophys. Acta* **1723**, 302–308
- Muir, R., Diot, A., and Poulton, J. (2016) Mitochondrial content is central to nuclear gene expression: Profound implications for human health. *Mol. Cell. Dev. Biol.* **38**, 50–156

35. Barazzoni, R., Short, K. R., and Nair, K. S. (2000) Effects of aging on mitochondrial DNA copy number and cytochrome c oxidase gene expression in rat skeletal muscle, liver, and heart. *J. Biol. Chem.* **275**, 3343–3347
36. Maute, R. L., Schneider, C., Sumazin, P., Holmes, A., Califano, A., Basso, K., and Dalla-Favera, R. (2013) tRNA-derived microRNA modulates proliferation and the DNA damage response and is down-regulated in B cell lymphoma. *Proc. Natl. Acad. Sci. U. S. A.* **110**, 1404–1409
37. Wang, M., Liu, H., Zheng, J., Chen, B., Zhou, M., Fan, W., Wang, H., Liang, X., Zhou, X., Eriani, G., Jiang, P., and Guan, M. X. (2016) A deafness and diabetes associated tRNA mutation caused the deficient pseudouridylation at position 55 in tRNA^{Glu} and mitochondrial dysfunction. *J. Biol. Chem.* **291**, 21029–21041
38. El Yacoubi, B., Bailly, M., and de Crécy-Lagard, V. (2012) Biosynthesis and function of posttranscriptional modifications of transfer RNAs. *Annu. Rev. Genet.* **46**, 69–95
39. Dogan, S. A., Pujol, C., Maiti, P., Kukat, A., Wang, S., Hermans, S., Senft, K., Wibom, R., Rugarli, E. I., and Trifunovic, A. (2014) Tissue-specific loss of DARS2 activates stress responses independently of respiratory chain deficiency in the heart. *Cell Metab.* **19**, 458–469
40. McFarland, M. R., Keller, C. D., Childers, B. M., Adeniyi, S. A., Corrigall, H., Raguin, A., Romano, M. C., and Stansfield, I. (2020) The molecular aetiology of tRNA synthetase depletion: Induction of a GCN4 amino acid starvation response despite homeostatic maintenance of charged tRNA levels. *Nucleic Acids Res.* **48**, 3071–3088
41. Zhang, J. (2020) Unboxing the T-box riboswitches-A glimpse into multivalent and multimodal RNA-RNA interactions. *Wiley Interdiscip. Rev. RNA* **11**, e1600
42. McManus, M. J., Picard, M., Chen, H. W., De Haas, H. J., Potluri, P., Leipzig, J., Towheed, A., Angelin, A., Sengupta, P., Morrow, R. M., Kauffman, B. A., Vermulst, M., Narula, J., and Wallace, D. C. (2019) Mitochondrial DNA variation dictates expressivity and progression of nuclear DNA mutations causing cardiomyopathy. *Cell Metab.* **29**, 78–90
43. Herbers, E., Kekäläinen, N. J., Hangas, A., Pohjoismäki, J. L., and Goffart, S. (2019) Tissue specific differences in mitochondrial DNA maintenance and expression. *Mitochondrion* **44**, 85–92
44. Johnson, D. T., Harris, R. A., French, S., Blair, P. V., You, J., Bemis, K. G., Wang, M., and Balaban, R. S. (2007) Tissue heterogeneity of the mammalian mitochondrial proteome. *Am. J. Phys. Cell Phys.* **292**, C689–C697
45. Fernandez-Vizarra, E., Enriquez, J. A., Perez-Martos, A., Montoya, J., and Fernandez-Silva, P. (2011) Tissue-specific differences in mitochondrial activity and biogenesis. *Mitochondrion* **11**, 207–213
46. King, M. P., and Attardi, G. (1993) Post-transcriptional regulation of the steady-state levels of mitochondrial tRNAs in HeLa cells. *J. Biol. Chem.* **268**, 10228–10237
47. Bayona-Bafaluy, M. P., Acín-Pérez, R., Mullikin, J. C., Park, J. S., Moreno-Loshuertos, R., Hu, P., Pérez-Martos, A., Fernández-Silva, P., Bai, Y., and Enriquez, J. A. (2003) Revisiting the mouse mitochondrial DNA sequence. *Nucleic Acids Res.* **31**, 5349–5355
48. Ji, Y., Nie, Z., Meng, F., Hu, C., Chen, H., Jin, L., Chen, M., Zhang, M., Zhang, J., Liang, M., Wang, M., and Guan, M. X. (2021) Mechanistic insights into mitochondrial tRNA^{Ala} 3'-end metabolism deficiency. *J. Biol. Chem.* **297**, 100816
49. Guan, M. X., Yan, Q., Li, X., Bykhovskaya, Y., Gallo-Teran, J., Hajek, P., Umeda, N., Zhao, H., Garrido, G., Mengesha, E., Suzuki, T., del Castillo, I., Peters, J. L., Li, R., Qian, Y., *et al.* (2006) Mutation in TRMU related to transfer RNA modification modulates the phenotypic expression of the deafness-associated mitochondrial 12S ribosomal RNA mutations. *Am. J. Hum. Genet.* **79**, 291–302
50. Yu, J., Liang, X., Ji, Y., Ai, C., Liu, J., Zhu, L., Nie, Z., Jin, X., Wang, C., Zhang, J., Zhao, F., Mei, S., Zhao, X., Zhou, X., Zhang, M., *et al.* (2020) PRICKLE3 linked to ATPase biogenesis manifested Leber's hereditary optic neuropathy. *J. Clin. Invest.* **130**, 4935–4946